Drift og vedlikehold
Fagressurs Drift og vedlikehold
Geofag Drift og vedlikehold
13.8.2024

Statens vegvesen

Sensors on UAVs for snow mapping

Recommendations for UAV sensor technologies for snow mapping and characterization

STATENS VEGVESENS RAPPORTER Nr. 996

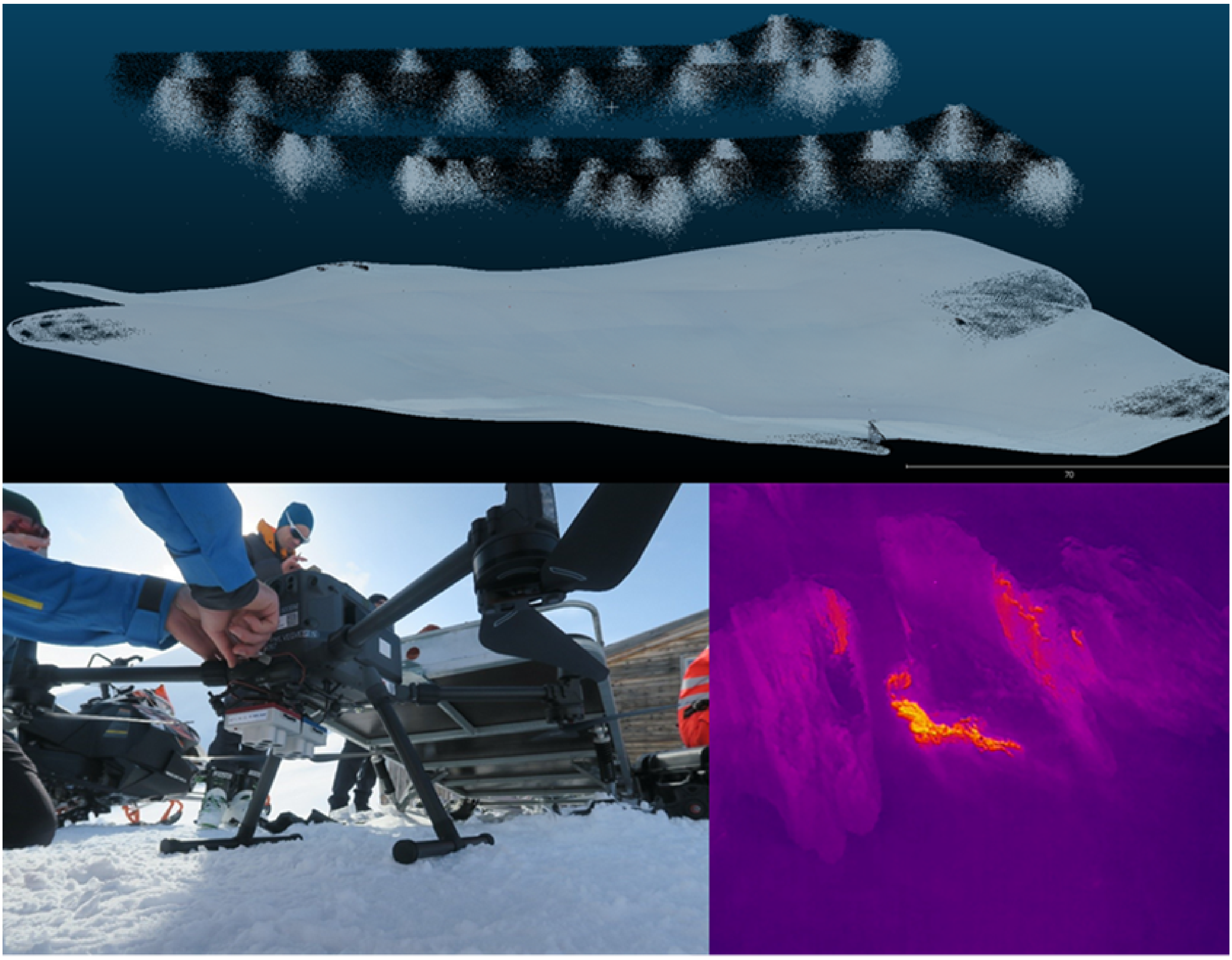

Illustration: GEOSFAIR project

Tittel
Sensors on UAVs for snow mapping

Undertittel
Recommendations for UAV sensor technologies for snow mapping and

Forfatter
Bastien Dupuy (editor) with co-authors from SINTEF, NGI and NPRA (see page 3)

Avdeling
Fagressurs Drift og vedlikehold

Seksjon
Geofag Drift og vedlikehold

Prosjektnummer
C15115

Rapportnummer
996

Prosjektleder
Tore Humstad

Godkjent av
Tore Humstad

Emneord
UAV, UAS, lidar, termofotografering, multispektrale bilder, fotogrammetri, georadar, snøskred, snø

Sammendrag
Prosjektet GEOSFAIR har som mål å forbedre Statens vegvesen sin kartlegging og vurdering av snøskredfare ved hjelp av ubemannede luftfartøysystemer (UAS eller droner). I fbratte fjellsider vil disse droner kunne samle data om snøoverflate og -egenskaper ved hjelp av spesialiserte sensorer. Disse dataene vil bli behandlet og analysert for å forbedre risikovurdering og beslutningstaking knyttet til geofarer.

Denne rapporten beskriver funnene fra arbeidspakke 1 (WP1) i prosjektet, som fokuserer på å utvikle optimale spesifikasjoner for UAS-flyplaner, sensorer og støtte for skredovervåking og -varsling.

Title
Sensors on UAVs for snow mapping

Subtitle
Recommendations for UAV sensor technologies for snow mapping and

Author
Bastien Dupuy (editor) with co-authors from SINTEF, NGI and NPRA (see page 3)

Department
O&M Planning and Engineering Services

Section
O&M Geomechanics

Project number
C15115

Report number
996

Project manager
Tore Humstad

Approved by
Tore Humstad

Key words
UAV, UAS, lidar, termofotografering, multispektrale bilder, fotogrammetri, georadar, snøskred, snø

Summary
The GEOSFAIR project aims to enhance the NPRA's geohazard risk assessments by using uncrewed aircraft systems (UAS) to monitor snow and danger of snow avalanches. In mountainous areas with steep slopes, these UAS will collect data on the snowpack using specialized sensors. This data will be processed and analyzed to improve risk assessment and decision-making for geohazards.

This report outlines the findings from Work Package 1 (WP1) of the project, which focuses on developing optimal specifications for UAS flight systems, sensors, and logistical support for avalanche forecasting and monitoring.

Antall sider 30

Pages 30

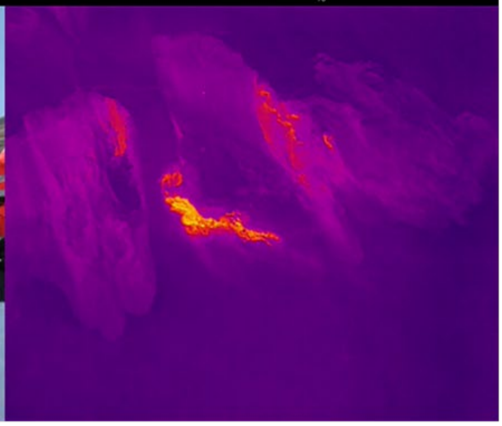

Report

GEOSFAIR (Geohazard survey from Air) deliverable D1.1

Recommendations for UAV sensor technologies for snow mapping and characterization

Authors:

Bastien Dupuy, Are Hellandsvik, Richard J. D. Moore, Trine Kirkhus, Asbjørn Berge (SINTEF), Halgeir Dahle, Emil Solbakken (NPRA), Elisabeth Hoffstad Reutz, Sean Salazar (NGI)

Clients and partners:

The research council of Norway, NPRA, NGI

SINTEF Industry
Postal address:
Postboks 4763 Torgarden
7465 Trondheim, Norway

Switchboard: +47 40005100

info@sintef.no

Enterprise /VAT No:
NO 919303808 MVA

Report

GEOSFAIR (Geohazard survey from Air) deliverable D1.1

Recommendations for UAV sensor technologies for snow mapping and characterization

KEYWORDS
Klikk eller trykk her for å skrive inn tekst.

VERSION
1

DATE
2024-08-13

AUTHORS
Bastien Dupuy, Are Hellandsvik, Richard J. D. Moore, Trine Kirkhus, Asbjørn Berge (SINTEF), Halgeir Dahle, Emil Solbakken (NPRA), Elisabeth Hoffstad Reutz, Sean Salazar (NGI)

CLIENTS AND PARTNERS
The research council of Norway, NPRA, NGI

CLIENT'S REFERENCE
321035/080

PROJECT NO.
102025034

NO. OF PAGES
27

SUMMARY
Abstract

PREPARED BY
Bastien Dupuy

SIGNATURE

CHECKED BY
Arnt Grøver

SIGNATURE

APPROVED BY
Peder Eliasson

SIGNATURE

COMPANY WITH MANAGEMENT SYSTEM CERTIFIED BY DNV
ISO 9001 • ISO 14001
ISO 45001

REPORT NO.	ISBN	CLASSIFICATION	CLASSIFICATION THIS PAGE
2024:00903	978-82-14-07002-6	Unrestricted	Unrestricted

Document history

VERSION	DATE	VERSION DESCRIPTION
1	2024-08-13	Final version

Table of contents

1 Introduction

The primary objective of the GEOSFAIR project is to improve geohazard risk assessment conducted by the NPRA, through the utilization of data collected by uncrewed aircraft systems (UAS). Specifically focusing on the hazards posed by snow avalanches, the UAS will operate in mountainous terrains with steep slopes, equipped with a sensor payload to gather crucial information from the accumulated snowpack. The collected data will undergo a comprehensive workflow of processing and analysis, to facilitate risk assessment and decision-making processes when dealing with geohazards.

This document summarizes the findings from work package 1 (WP1) within the GEOSFAIR project. WP1 aims to provide optimal user-guided specifications for the UAS flight system, the associated sensors, and the logistical aspects necessary to forecast and monitor avalanches, as well as relevant snow parameters in adverse weather conditions. An initial mapping of relevant snow and avalanche properties and their potential value to NPRA avalanche forecasting is summarized in Figure 1. It includes some information about sensors being operationally used today, and suggestions for other relevant sensors. To complement this initial study, a state-of-the-art review has been performed as part of the GEOSFAIR project[1]. This review summarizes the research on several topics related to UAS-borne sensor technologies, and complements the recommendations contained in this document.

Figure 1 (next page): mapping of snow and avalanche properties relevant for NPRA avalanche forecasting and suggested UAV sensors to record information on these properties.

[1] McCormack E. et al. (2024), Avalanche Hazard Assessment Supported by UAS, Statens Vegvesen report, 958.

Snow, avalanche and terrain properties relevant to NPRA avalanche forecasting and UAS sensoring

Evaluation of usage and information value to guide the development of new sensors

When is data relevant for different avalanche problems?
B - **Before** avalanche/avalanche hazard situation
D - **During** avalanche/avalanche hazard situation
A - **After** avalanche/avalanche hazard situation

(spot) - Information can be "sampled" at one or more spots within the relevant area

WL - Weak layer

Category (Information class)	Target element	Target property	Target description	Key applications	Nysnø (storm slab, dry loose avalanches)	Fokksnø (wind slab)	Vedvarende svakt lag (persistent/deep persistent slab)	Våt snø (wet slab, wet loose avalanches)	Glideskred (glide slab)	Area of interest	Information value	Information availability with current methods	Current methods (operationally used by NPRA)	Suggested sensors relevant for UAS	Known challenges
Avalanches	Snow surface	Location	3D surface mapping	• Analyse lengths, heights and volumes of avalanches • Document natural avalanches • Document effect of active avalanche control (before/after)	D,A	D,A	D,A	D,A	D,A	Release area, track, runout zone	High	Moderate	UAS SfM (VIS) UAS Lidar Doppler radar Satellite imagery	VIS, NIR, Lidar	• Visibility, wind, drifting snow and precipitation during storms
		Structure	2D/3D surface mapping Recognition of surface features in avalanche starting zone/track/runout zone	• Map recent avalanche activity and avalanche cycles • Classify avalanches (types, phases)	D,A	D,A	D,A	D,A	D,A	Release area, track, runout zone	Moderate	Moderate	Manual observations Stationary cameras (VIS/IR) UAS SfM (VIS) UAS Lidar	VIS, NIR, IR, Lidar	• Visibility, wind, drifting snow and precipitation during storms
		Thermal radiation	Measure differences in thermal radiation between avalanche path/debris and unaffected snow	• Map recent avalanche activity in poor weather/light conditions	D	D	D	D	D	Release area, track, runout zone	Moderate	Low	Stationary cameras (IR)	IR	• Rapid adaptation of snow surface temperature to air temperature in cloudy conditions • Drifting snow and precipitation particles in the air during storms
Snowpack	Snow surface	Location	3D surface mapping	• Measure snow depth/volumes (e.g. to estimate potential avalanche size) • Change detection (change due to loading, erosion, settlement, melting etc.)	D	B,D	B,D	B,D	B,D	Release area, track, runout zone	High	Moderate	UAS SfM (VIS) UAS Lidar	VIS, NIR, Lidar	• Visibility, wind, drifting snow and precipitation during storms
		Structure	2D/3D surface mapping	• Recognition of surface features (sastrugis, cornices, drainage patterns, glide cracks etc.) • Detection of surface movement (glide/creep)		B,D		B,D	B,D	Release area	Moderate	Moderate	Manual observations Stationary cameras (VIS/IR) UAS images/SfM (VIS) UAS Lidar	VIS, NIR, Lidar	• Visibility, wind, drifting snow and precipitation during storms
		Grain properties	Identify surface grain type and grain size	• Evaluate snowpack build-up • Identify and map surface hoar and facets (forming persistent weak layers if buried) • Identify crust/melt forms	B	B	B			Release area (spot)	Moderate	Low	Extrapolation from nearest manual observations	NIR	• Grain properties at the surface may have very high spatial variability
		Hardness	Measure/estimate surface hardness/cohesion	• Identify crust and wind-affected snow • Identify avalanche entrainment potential • Identify loose snow available for wind transport	B	B	B			Release area (spot), path, crest/plateau	Low	Low	Extrapolation from nearest manual observations	Penetrometer?	• Penetration of hard snow layers requires a lot of force • Risk of instrument getting stuck
		Temperature	Measure snow surface temperature	• Evaluate surface or near-surface temperature gradients and metamorphism processes	B	B	B	B	B	Release area (spot)	Low	Low	Extrapolation from nearest manual observations	IR	
		Water content	Measure wetness/water content at the snow surface	• Indicator of sub-surface water content				D		Release area (spot)	Moderate	Low	Extrapolation from nearest manual observations	NIR	
		Thermal radiation	Identify local variations in thermal radiation	• Identify areas of ongoing or recent wind deposition • Map relative snow depth		D	D			Release area	Low	Low	Not used	IR	• Temperature difference between blowing snow and snow on the surface is usually small
	Sub-surface snow	WL hardness	Measure/estimate weak layer hardness/cohesion	• Evaluate stability (weak layer strength, ease of triggering, fracture propagation potential)		D	B,D	B		Release area (spot)	High	Low	Extrapolation from nearest manual observations	GPR	• Very high vertical resolution required
		WL grain properties	Identify weak layer grain type and grain size	• Evaluate stability (weak layer strength, weak layer load, ease of triggering, fracture propagation potential)		D	B,D	B		Release area (spot)	High	Low	Extrapolation from nearest manual observations	GPR	• Very high vertical resolution required
		WL density	Measure/estimate weak layer density	• Evaluate stability (weak layer strength, ease of triggering, fracture propagation potential)		D	B,D	B		Release area (spot)	Moderate	Low	Not used	GPR	• Very high vertical resolution required
		WL thickness	Measure thickness of weak layer	• Evaluate stability (weak layer strength, ease of triggering, fracture propagation potential)		D	B,D	B		Release area (spot)	High	Low	Extrapolation from nearest manual observations	GPR	• Very high vertical resolution required
		WL depth	Measure depth to weak layer	• Evaluate stability (weak layer load, ease of triggering, fracture propagation potential)		D	B,D	B		Release area (spot)	High	Low	Extrapolation from nearest manual observations	GPR	
		Slab hardness	Measure/estimate hardness/cohesion of snow above WL	• Evaluate stability (ease of triggering, fracture propagation potential)	D	D	B,D	B		Release area (spot)	High	Low	Extrapolation from nearest manual observations	GPR Penetrometer? Green lidar?	
		Slab density	Measure/estimate density of snow above WL	• Evaluate stability (weak layer load, ease of triggering, fracture propagation potential)	D	D	B,D	B		Release area (spot)	Moderate	Low	Not used	GPR Penetrometer? Green lidar?	
		Water content	Measure wetness/water content, detect drainage channels and water collection above impermeable interfaces	• Evaluate stability (weak layer strength reduction due to wettening, weak layer load, friction on gliding surfaces) • Evaluate probability of slush flows	B, D, A			B,D	B,D	Release area (spot)	High	Low	Extrapolation from nearest manual observations	GPR Green lidar?	• Water content is very dependant on local topography
		Temperature	Measure temperature distribution in the snowpack	• Detect strong temperature gradients, causing faceting • Evaluate general metamorphism processes • Identify isothermal snowpacks			B,D	D	D	Release area (spot)	Moderate	Moderate	Extrapolation from nearest manual observations SM4	Penetrometer with temp. sensors?	
	Ground	Location/depth	Direct mapping of snow depth	• Evaluate general snow depth distribution						Release area, track	Low	Moderate		GPR	
Terrain	Ground	Location	3D surface mapping on snow free ground	• Calculation of snow depth • Calculation of slope angle, curvature and terrain roughness • Run-out simulations	B	B	B	B	B	Release area, track	High	High	Airborne Lidar UAS SfM (VIS) UAS Lidar	VIS Lidar	

SINTEF

2 LiDAR – Light Detection and Ranging

2.1 Description

LiDAR, or "Light Detection and Ranging", is a method that determines the distance from a laser source to a targeted object by measuring the time for the reflected light to return to the receiver. Measurements in different directions generate a 3D-representation of a surface, referred to as LiDAR scanning. LiDAR technology can be used stationary or be carried over land or in the air while performing measurements. Over the years, the LiDAR-sensor has become lighter and can now be carried by an UAS. LiDAR-measurements from drones are typically performed to collect 3D-representations of smaller areas, while larger areas are usually mapped by airplane. UAS-carried LiDAR measurements are relatively low cost and make it possible to perform repeated surveys efficiently.

2.2 Measurement Principle

Airborne LiDAR system consists of three parts:

- Laser scanner unit (LiDAR)
- IMU (inertial measurement unit): Unit to measure and report specific gravity and angular rate (pitch, roll and yaw) to an attached object, for example a LiDAR scanner.
- GPS unit with real time error corrections, provides an absolute position of the LiDAR system.

The system connected to an airplane is illustrated in Figure 2. Together, the system will provide a 3D representation of the targets' surface.

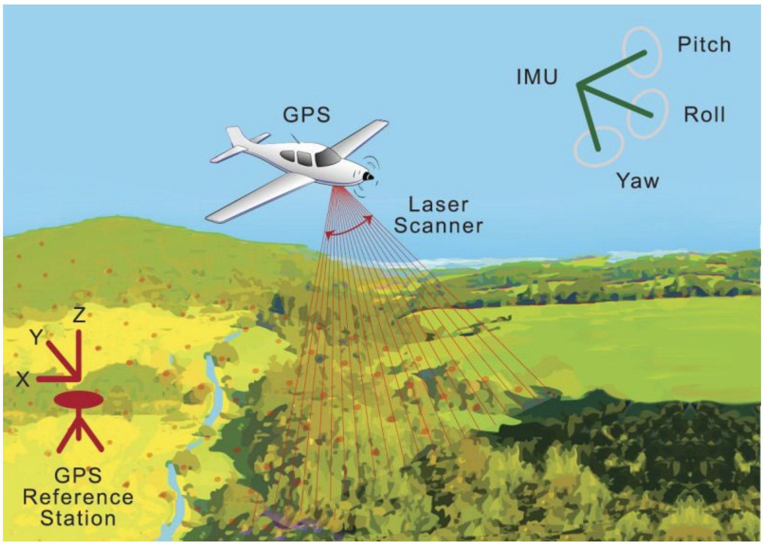

Figure 2: Basic principles for airborne LiDAR data collection (figure from Spectra Physics[2])

LiDAR wavelength for surveying onshore topography is near infrared light (typically 905 nm) or infrared light (typically 1064 nm), while bathymetric LiDAR uses water penetrating green light to measure riverbeds and seafloor (typically 532 nm).

Each light pulse can be reflected multiple times. Multiple returns occur when a pulse strikes a target, but is not completely reflected or absorbed, resulting in a portion of the pulse continuing to lower objects where

[2] https://www.spectra-physics.com/en/

it can also be reflected. Multiple returns make a larger dataset and generate 3D structures of trees, vegetation and constructions.

2.3 Operational Requirements

Carrying a LiDAR system on a UAS is limited by the weather requirements to the drone. These requirements are temperature, wind speed and precipitation. The LiDAR system itself may have weather requirements on temperature and precipitation. Precipitation during data capture generates return pulses from snowflakes or water drops.

The number of pulses emitted from the LiDAR system pr second is constant during flight, ranging from tens of thousands to millions. Point density on the ground depends on the number of pulses, flight height and flight speed. For topographic mapping the point density needed is from 2-10 points pr square meter.

2.4 Experimental Results

GEOSFAIR performed a vendor test of LiDAR sensors carried by UAS[3] to support avalanche monitoring. Seven vendors (drone operators) and the NPRA acquired data from LiDAR sensors over field sites of varying complexity. The resulting datasets were analyzed for accuracy and for usability for avalanche hazard assessment.

The vendor test demonstrated that, in general, the LiDAR datasets were acquired with a level of precision and accuracy that could be used for monitoring of the snowpack and avalanche risk. When combined with bare earth elevation data, the LiDAR data can be used to determine snow depth and snow volume, and with repeated flights, could also track changes in the snowpack. The LiDAR returns also provided usable information on the surface of the snowpack and of the surrounding terrain. The use of UAS for avalanche monitoring on an operational level depends on the ability of the aircraft to fly and to collect data in a range of weather conditions and in rugged terrain, so there is some uncertainty on how well LiDAR data can be collected routinely and operationally in all situations.

The demonstration highlighted room for improvement in the collection of UAS LiDAR data. Even the surveying professionals at this demonstration, at times, produced inaccurate or sub-optimal results and some results showed signs of systematic errors. This suggests a successful LiDAR data collection operation will require detailed knowledge of the technology (both of the UAS and the LiDAR), good referencing systems, extensive testing, and efficient survey workflows.

LiDAR measurements in active precipitation (e.g. snowing) conditions are not ideal for data acquisition. The first return will, for many laser beams, be reflected from the snow crystals in the air. In light snowfall, the result may be satisfactory after post-processing (Figures 3 and 4).

[3] Solbakken E. et al. (2021), Lidar on UAS to support avalanche monitoring. Findings from demonstration in Trollstigen, Statens vegvesen report, 825.

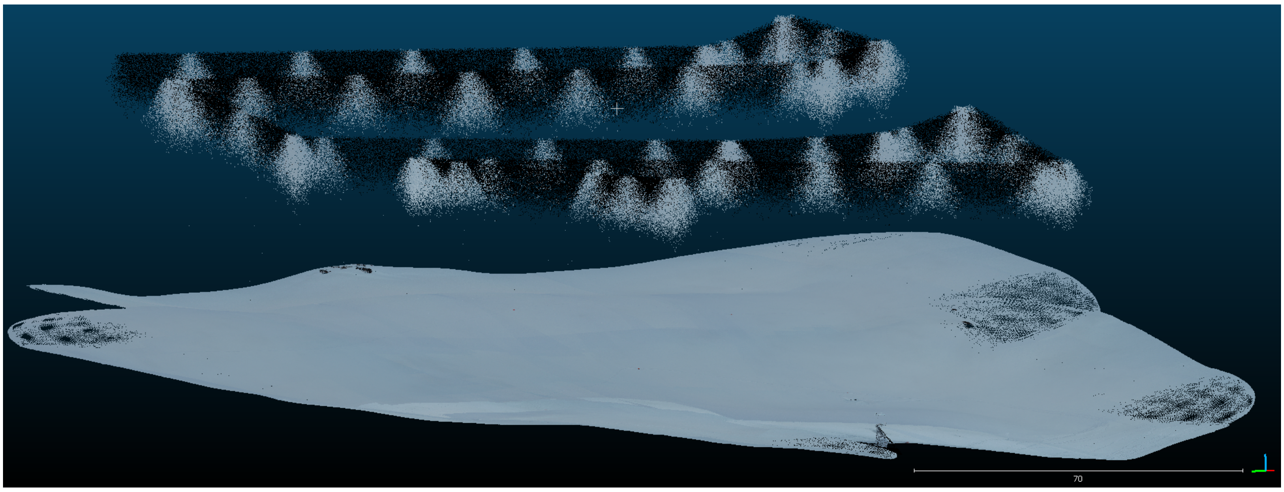

Figure 3: LiDAR point cloud acquired in light snowing condition.

Figure 4: Hill-shaded terrain model (0,1x0,1 m cell size) based on the point cloud depicted in Figure 3.

3 Thermal Imaging

3.1 Description

Thermal imaging is a non-destructive and a non-contact method of gaining information about thermal properties, enabling continuous detection of heat distribution on the surface of a target. A thermal camera sensor records the emitted longwave infrared radiation from the surface of an object. The resulting image enables one to visualise surface temperatures and thermal gradients. Thermal cameras can be used as a hand-held sensor but can also be attached to a UAS to e.g., map the temperature gradient over a larger area.

3.2 Measurement Principle

In contrast to conventional (visible light) cameras, thermal cameras are sensitive to the longwave infrared region, located between the visible light and microwave frequency, on the electromagnetic spectrum (Figure 5). The sensor exploits the fact that everything above absolute zero emits infrared radiation. In general, the higher the temperature of an object, the more energy is emitted[4]. The thermal camera measures this emitted infrared radiation from the target, its so-called heat signature.

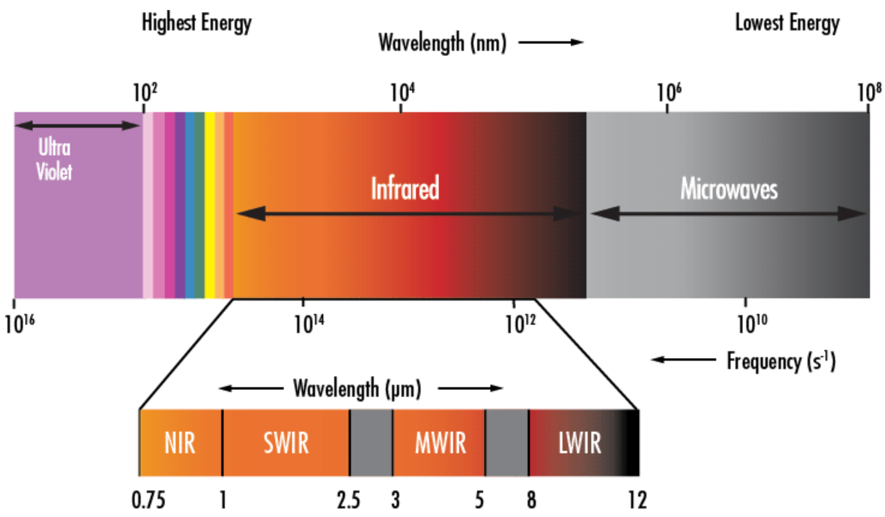

Figure 5: Electromagnetic spectrum illustrating longwave infrared (LWIR) wavelength range (figure from Edmund Optics[5]).

A thermal camera consists of infrared detectors, processing electronics and a system to acquire the images. The detector absorbs the emitted radiation form the object, converting it into electrical signals[6]. Instead of displaying the intensity of these signals, they are converted into a colourmap, visualizing the temperature (Figure 6).

[4] Prakash, A. (2000), Thermal Remote Sensing: Concepts, Issues and Applications, International Archives of Photogrammetry and Remote Sensing, Vol. 33, pp. 239-243.
[5] Edmund Optics, 2012.
[6] ElMasry G. et al. (2020), Emerging thermal imaging techniques for seed quality evaluation: Principles and applications, Food Research International, Vol. 131, doi:10.1016/j.foodres.2020.109025.

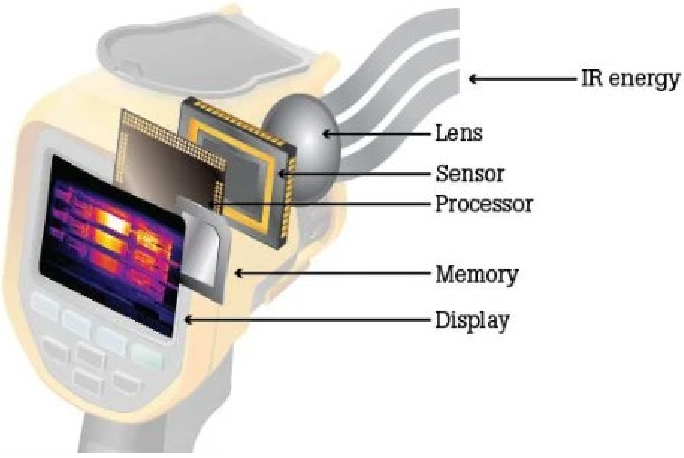

Figure 6: Basic principle of how a thermal camera works (figure from Fluke[7]).

3.3 Operational Requirements

The quality of the thermal imaging system is affected by the image and intensity resolution, thermal sensitivity, and scan speed. The radiation that the thermal camera detects may be affected by the environmental conditions, like ambient temperature and relative humidity[8,9]. Within the GEOSFAIR project, both hand-held and UAS-carried thermal imaging cameras were field tested in cold environments. Measurement targets included snow-surfaces (snow pit observations and airborne surveys) and were correlated with temperatures measured with conventional thermometers.

3.4 Experimental Results

The field tests were performed using thermal imaging cameras of the type DJI H20T (UAS-carried, airborne) and Fluke Ti-400 (hand-held, on ground). Surface temperatures were recorded for each pixel within the thermal images. In addition to measuring snow surface temperatures over larger areas by UAS (see examples in Figure 7), thermal images were collected on snow pit surfaces, using the Fluke Ti-400 series hand-held camera, as illustrated in Figure 8.

The tests revealed that the collected thermal images from both the hand-held and the UAS-mounted thermal cameras provided results that generally correlated well with measured surface temperatures using a conventional thermometer. However, the temperatures in the UAS images were not validated in many different areas, rather they were interpreted qualitatively. The value of the thermal images collected using both methods was most clear in highlighting thermal gradients and relative temperature differences, rather than absolute temperature measurements. Moreover, thermal images collected by UAS may provide value in conditions with little to no (sun)light.

[7] "How infrared cameras work", Fluke, www.fluke.com/en/learn/blog/thermal-imaging/how-infrared-cameras-work. Accessed 10 February 2023

[8] Ishimwe, R. et al. (2014), Applications of Thermal Imaging in Agriculture – A Review, Advances in Remote Sensing, Vol. 3, pp. 128-140, doi:10.4236/ars.2014.33011.

[9] ElMasry G. et al. (2020), Emerging thermal imaging techniques for seed quality evaluation: Principles and applications, Food Research International, Vol. 131, doi:10.1016/j.foodres.2020.109025.

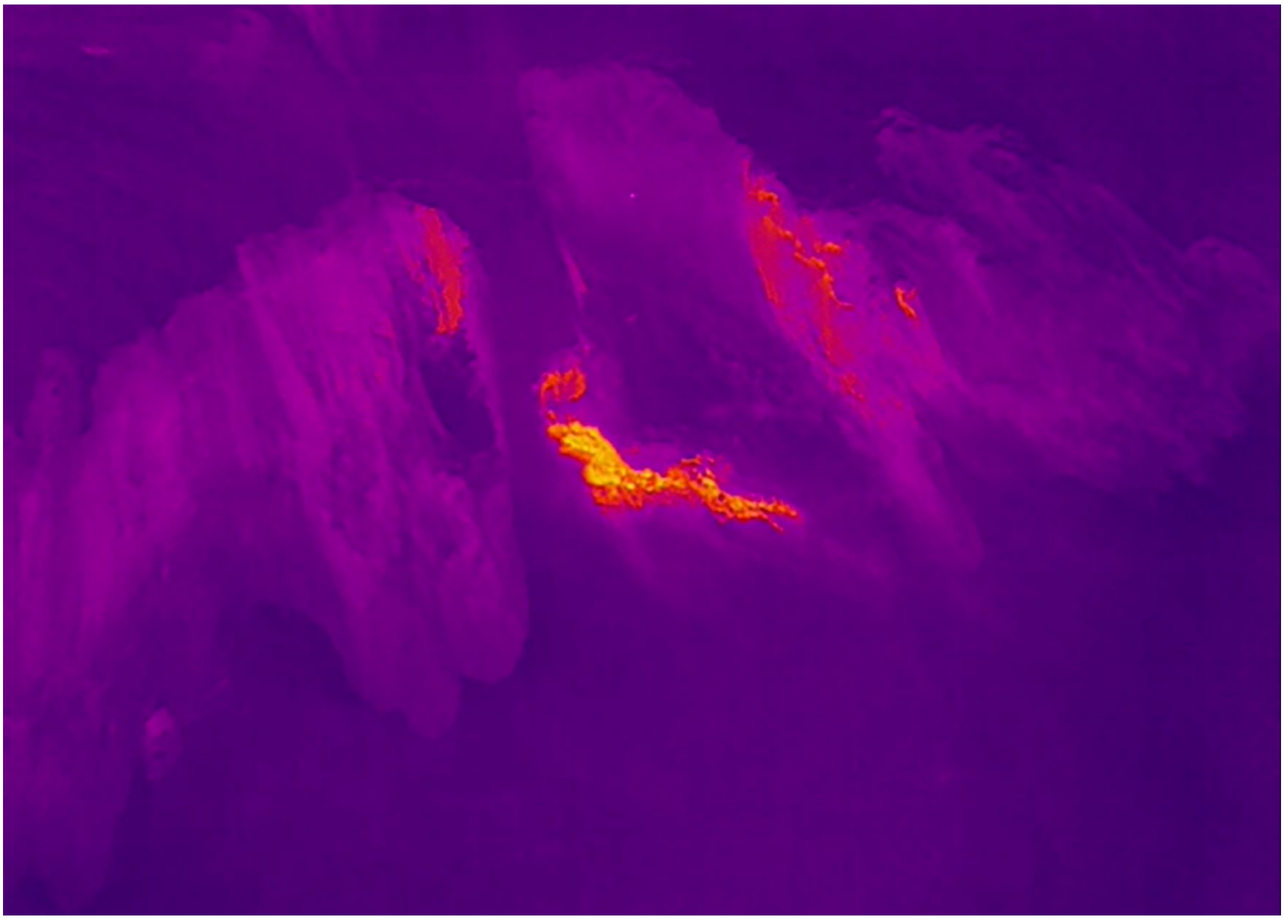

Figure 7: Examples of thermal camera images captured while performing artificial release of snow avalanche by explosives. The camera is a UAS-carried DJI H20T camera; color-scale is relative to maximum measured temperature range in each image subset.

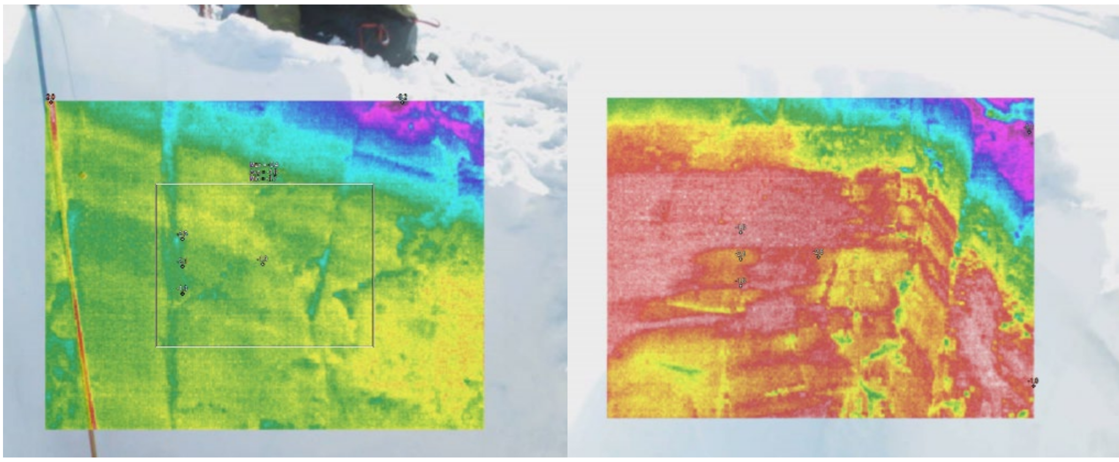

Figure 8: Examples of thermal camera images captured with the hand-held Fluke instrument; color-scale is relative to maximum measured temperature range in each image subset.

4 Multi-Spectral Imaging

4.1 Description

Multi-spectral cameras produce images within certain wavelength ranges across the electromagnetic spectrum, including light beyond the visible light range, i.e., infrared and ultraviolet. Spectral imaging is used for remote sensing to get more information from the earth's surface. It is widely used to characterize vegetation. Using drones to gather similar data below the clouds and with finer spatial details is also commercially available.

Flying a spectral camera on UASs is a possible sensor for inspecting larger areas to determine the surface's snow type. This information over time during a winter season might be used to build a model of the layers in the snowpack. The question is whether the information from these spectral bands contain relevant information to predict whether a snow layer currently on top might become a weak layer in the snowpack over time.

4.2 Measurement Principle

Multi spectral cameras considered here are passive in the sense that they do not illuminate the scene. The sun is providing light with the spectra of black body radiation. The camera is measuring/imaging the reflected light from the surfaces at several distinct wavelengths both visual and beyond the visual spectrum.

It has been shown[10,11] that there is a wavelength shift dependent on the grain size of the snow (Figure 9). These measurements are from satellites. UAVs multispectral cameras often use the same wavelengths as seen relevant in remote sensing for monitoring vegetation. Tables 1-4 give wavelengths in Sentinel satellites and in the MicaSense multispectral cameras designed for drones.

[10] Deems JS. et al. (2013), Lidar measurement of snow depth: a review. Journal of Glaciology, Vol. 59(215), pp. 467-479, doi:10.3189/2013JoG12J154
[11] Bühler Y. et al. (2011), Continuous, high resolution snow surface type mapping in high alpine terrain using WorldView-2 data, Digital Globe.

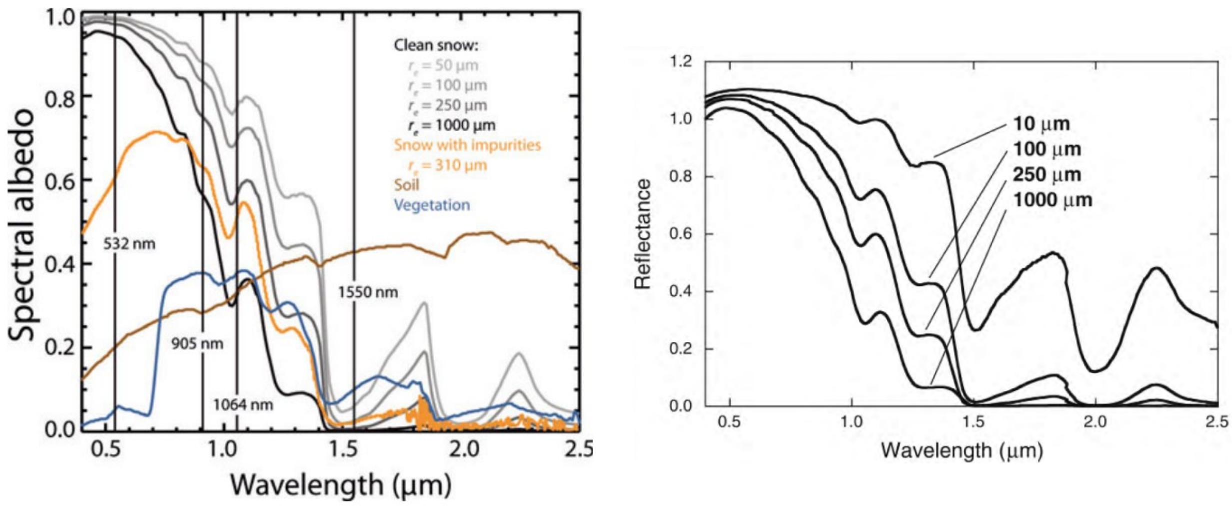

Figure 9: Reflected light as function of snow grain size, measured from satellite. Showing (L) effect of impurities[12] and (R) snow grain size[13].

Wavelengths and Bandwidths of the three Spatial Resolutions of the MSI instruments

Spatial Resolution (m)	Band Number	S2A		S2B	
		Central Wavelength (nm)	Bandwidth (nm)	Central Wavelength (nm)	Bandwidth (nm)
10	2	492.4	66	492.1	66
	3	559.8	36	559.0	36
	4	664.6	31	664.9	31
	8	832.8	106	832.9	106
20	5	704.1	15	703.8	16
	6	740.5	15	739.1	15
	7	782.8	20	779.7	20
	8a	864.7	21	864.0	22
	11	1613.7	91	1610.4	94
	12	2202.4	175	2185.7	185
60	1	442.7	21	442.2	21
	9	945.1	20	943.2	21
	10	1373.5	31	1376.9	30

Table 1: Sentinel satellite's spatial and spectral resolution (from Sentinel 2[14]).

[12] Deems, J.S., Painter, T.H. and Finnegan, D.C. (2013) 'Lidar measurement of snow depth: a review', Journal of Glaciology, 59(215), pp. 467–479. doi:10.3189/2013JoG12J154.

[13] Bühler, Y., Meier, L. and Meister, R., 2011. Continuous, high resolution snow surface type mapping in high alpine terrain using WorldView-2 data. Digital Globe.

[14] https://sentiwiki.copernicus.eu/web/s2-mission

File suffix	Band name	Center wavelength (nm)	Bandwidth (nm)
1	Blue	475	32
2	Green	560	27
3	Red	668	14
5	Red Edge	717	12
4	Near IR	842	57

Table 2: Spectral channels for RedEdge-MX with serial numbers RX02 or higher. Red camera (from Micasense[15]).

File suffix	Band name	Center wavelength (nm)	Bandwidth (nm)
6	Coastal Blue	444	28
7	Green	531	14
8	Red	650	16
9	Red Edge	705	10
10	Red Edge	740	18

Table 3: Spectral channels for RedEdge-MX Blue (in the Dual Camera System (from Micasense[16]).

File suffix	Band name	Center wavelength	Bandwidth
1	Blue	475 nm	32 nm
2	Green	560 nm	27 nm
3	Red	668 nm	16 nm
5	Red edge	717 nm	12 nm
4	Near infrared	842 nm	57 nm
6	Panchromatic	634.5 nm	463 nm
7	LWIR (Thermal)	10.5 µm	6 µm

Table 4: Spectral channels for MicaSense Altum-PT thermal camera (from Micasense[17]).

4.3 Experimental Results

The MicaSense RedEdge-MX is UAS flight ready and is primarily developed for inspecting farm fields by UAS. We have tested this sensor at Fonnbu spring 2022 by using NPRA's DJI Matrice 300 RTK (Figure 10). The conclusion from this is that we need to have control of the in-situ snow conditions, and to reproduce the results on estimating grain size from satellite data, we need to test the workflow on a variety of snow types and grain sizes.

[15] https://support.micasense.com/hc/en-us/articles/214878778-What-is-the-center-wavelength-and-bandwidth-of-each-filter-for-MicaSense-sensors

[16] https://support.micasense.com/hc/en-us/articles/214878778-What-is-the-center-wavelength-and-bandwidth-of-each-filter-for-MicaSense-sensors

[17] https://support.micasense.com/hc/en-us/articles/214878778-What-is-the-center-wavelength-and-bandwidth-of-each-filter-for-MicaSense-sensors

Figure 10: the MicaSense multispectral camera mounted on NPRA's DJI Matrice 300. An external GPS receiver was also mounted on the UAS for geotagging multispectral data. The camera was controlled directly from the ground via WiFi interface. (Photo: Tore Humstad)

4.4 Recommended future activities

How to parameterize the snow types efficiently to use for making models? We are still not sure whether we had large enough spread in snow types to determine how the spectral data is able to discriminate between snow types.

Identifying which factors influence the data other than snow type, e.g., terrain inclination angle, sun's incident angle and characterizing their effect/s will be an important outcome of analysis of the data captured at Fonnbu. Ideally, we wish to remove the effects of all other parameters other than the snow type.

Future work will include developing a modular sensor package and analysis pipeline that will enable simpler data capture and in-field validation and inspection of data captured.

5 Photogrammetry
5.1 Description

Structure-from-Motion (SfM) photogrammetry is a technique used to reconstruct three-dimensional scenes and high-resolution topographic data from 2D images. The technique may be applied to images that are obtained from drones and consumer-grade cameras and processed using freely available software. Unlike conventional photogrammetry, SfM does not require prior information about the camera location and orientation, nor the use of multiple control points. Instead SfM algorithms simultaneously solve the camera position and orientation (so called camera pose), and geometry of the scene by matching automatically identified features from multiple overlapping images taken from different perspectives[18].

5.2 Measurement Principle

The SfM feature extraction and algorithms need a set of multiple overlapping images taken from different orientations (e.g. as depicted in Figure 11). First, features in each image (key points) are identified and assigned a unique identifier. These features are invariant to the image scale and perspective. An algorithm is then used to identify corresponding key-points between the different images, based on criteria to filter and remove outliers. Then a bundle adjustment algorithm estimates the geometry of the scene and information about the camera location and orientation, simultaneously. The bundle adjustment minimizes the reprojection errors by optimizing the camera position and 3D structure. This creates a sparse point cloud consisting of the key points. The point cloud can then be georeferenced by using ground control points, and/or adding coordinates to the camera positions. Without georeferencing information, the point cloud will be referenced in a local coordinate system. A denser point cloud can be generated by filling in points in the point cloud[19].

Figure 11: SfM requires multiple overlapping photographs taken from different orientations with regards to the target, to create a 3D scene (figure from Westoby et al., 2012).

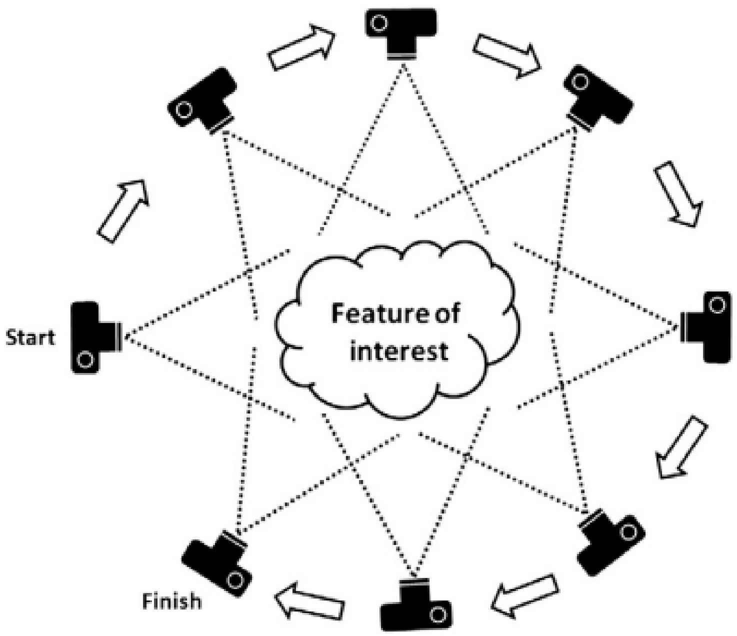

[18] Westoby, M.J. et al. (2012), 'Structure-from-Motion' photogrammetry: A low-cost, effective tool for geoscience applications, Geomorphology, Vol. 179, pp. 300-314, doi:10.1016/j.geomorph.2012.08.021.
[19] Smith, M.W. et al. (2016), Structure from motion photogrammetry in physical geography, Progress in Physical Geography, Vol. 40, No. 2, pp. 247-275, doi:10.1177/030913331561580.

5.3 Operational Requirements

SfM algorithms rely on key points that are visible in several images, hence they are dependent on the overlap between images, the resolution of the images and the texture of the surfaces in the scene. The precision and accuracy of the point cloud generated by SfM is influenced by the distance between the camera and its target, as a shorter distance generates an image with a relatively higher spatial resolution (Westoby et al., 2012 and Smith et al., 2016). As a minimum requirement, key points need to be visible in at least three images. However, as many as possible is recommended, and the coverage should be uniform (Westoby et al., 2012).

Testing of SfM algorithms in GEOSFAIR revealed that to obtain high quality photogrammetry results, the UAS had to be flown using effective terrain-following flight paths with suitable image overlap and flight altitude.

5.4 Experimental Results

In GEOSFAIR, several different platforms were used to collect images that were used to reconstruct terrain surfaces using SfM photogrammetry (as illustrated in Figure 12); including the DJI Mavic 2 Pro and DJI Phantom 4 RTK with integrated camera systems, the QuantumSystems Trinity F90+ with Sony RX1RII camera, and the DJI Matrice 300 RTK with Zenmuse P1 and L1 camera systems. In general, the results generated with the use of SfM provided accurate information about snow heights and the nature of the snow surface.

Some challenges were also experienced during the tests that affected the photogrammetry results, due to noise and non-matching images caused by lack of recognisable surface features, and problems with GNSS positioning errors. The SfM-technique on snow surfaces generally requires pictures to be taken in good light conditions to detect surface structures, and thereby generate a representative 3D-model.

Figure 12: illustration of a sparse point cloud generated with SfM photogrammetric reconstruction.

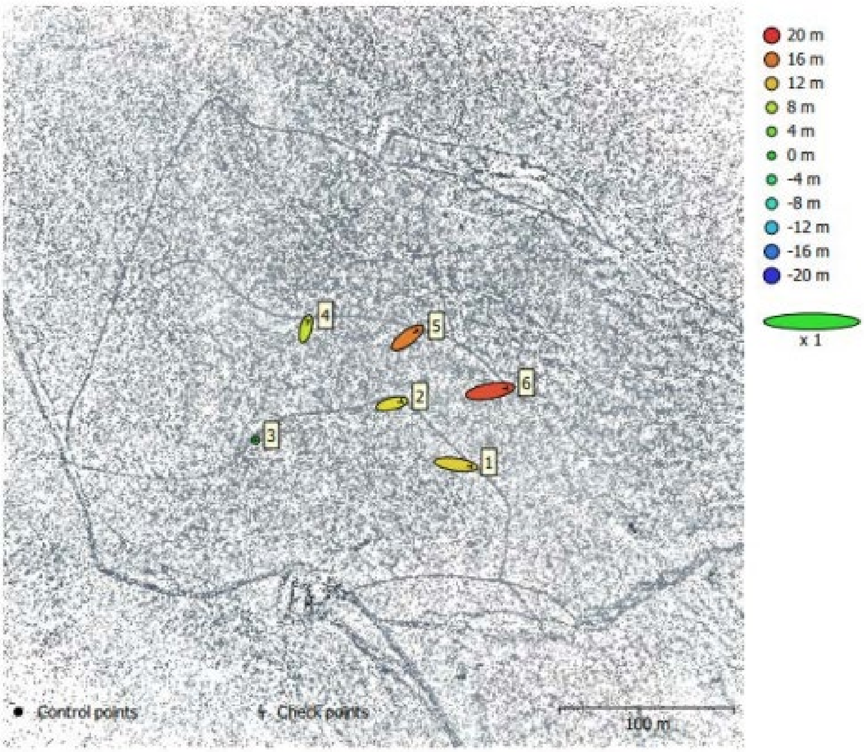

6 Ground Penetrating Radar

6.1 Description

GPR is standing for Ground Penetrating Radar and is a conventional sensor for underground/subsurface investigations. GPR is usually used on or very close to the ground, mounted on a cart, on a vehicle or towed manually. Recent development of lighter systems and antennas allow to mount it on commercial drones with a sufficient payload capacity. Typical results of GPR surveys are 2D profiles and images highlighting the underground structure and features. To some extent, properties of the subsurface can also be derived from GPR results.

6.2 Measurement Principle

6.2.1 GPR principles and Maxwell equations

GPR can be seen as an analogy to seismic surveys. Instead of mechanical waves, the GPR antenna is generating electromagnetic waves (EM). Maxwell equations are the constitutive equations controlling the electromagnetic wave propagation. Numerous detailed explanations of Maxwell equations can be found online[20,21,22]and in the literature[23]. The GPR wave velocity can be approximated by:

$$V = \frac{c}{\sqrt{\mu_R \epsilon_R}}$$

where μ_R and ε_R are the magnetic permeability and dielectric permittivity relative to free space values. *c* is the wave velocity of light and is a constant equal to $c = 3 * 10^8\ m/s$. If the propagation material is non-magnetic (such as snow), $\mu_R = 0$ and the velocity equation summarizes to:

$$V = \frac{c}{\sqrt{\epsilon_R}}$$

With *c* being a constant, the wave velocity is only dependent on relative permittivity ε_R.

6.2.2 Resolution and penetration depth

Due to wave propagation geometrical spreading, higher frequencies are more attenuated and propagate less deep and far. This does not account for intrinsic attenuation which is assumed to be negligible in highly resistive material like snow and ice. Penetration depth is to some extent related to skin depth of the EM waves. Skin depth is defined as the depth where the amplitude of sinusoidal EM wave is reduced to 37% of its original amplitude. For high frequency regime, the skin depth δ can be formulated as:

$$\delta = 0.0053 \frac{\sqrt{\epsilon_R}}{\sigma}$$

where σ (S/m) is the conductivity. Basically, the skin depth, i.e. the penetration depth, is larger in materials with lower conductivities and/or in materials with higher dielectric permittivities. Penetration depth

[20] https://en.wikipedia.org/wiki/Maxwell%27s_equations
[21] https://gpg.geosci.xyz/content/GPR/GPR_fundamental_principles.html
[22] https://www.eoas.ubc.ca/courses/eosc350/content/methods/gpr-06.htm
[23] Carcione, J. M. (2007), *Wave fields in real media: Wave propagation in anisotropic, anelastic, porous and electromagnetic media. Elsevier.*

(probing distance) is usually assumed to be 3 times the skin depth and it is the depth where the GPR can be used to get information about underground medium. Following the skin depth equation, the penetration depth D is expressed:

$$D = 3\delta = 0.0159\frac{\sqrt{\epsilon_R}}{\sigma}$$

For snow layers, as the electrical conductivity σ tends towards zero, the penetration depth D is assumed to be very large and will only be affected by geometrical spreading.

On the other hand, the resolution is dependent on wavelength, itself dependent on wave frequency and velocity. The EM wavelength λ is calculated by:

$$\lambda = \frac{c}{f\,\sqrt{\epsilon_R}}$$

The vertical resolution is in ideal conditions equal to tenth of the wavelength. In real cases, it is assumed that the vertical resolution is between one-third and one-tenth of the wavelength. The thickness of a layer must be at least one-fourth of the wavelength of the signal to be resolved. Table 5 gives the expected minimum and maximum resolutions depending on different snow layers.

	Frequency	1000 MHz		
	ε_R	λ (cm)	Resolution min (cm)	Resolution max (cm)
Rounded grains	1,80	22,4	7,5	2,2
Dense snow	2,20	20,2	6,7	2,0
Facets or precipitation particles	1,16	27,9	9,3	2,8

Table 5: example of expected min and max resolution calculated for different type of snow at 1GHz frequency.

There is a trade-off between resolution and penetration depth. For the same medium, better resolution is obtained by increasing the antenna frequency, but this will decrease penetration depth. On the other side, penetration depth can be increased by lowering down the antenna frequency, but this decreases the resolution.

6.2.3 Snow density models for permittivity

Dry snowpack and wet snowpack (i.e. with liquid water inside the snow) have different EM properties. Dry snow conductivity is assumed to be 0, that means that the permittivity is not a complex number and consequently the intrinsic attenuation is negligible, while wet snow conductivity is of the order of 0.001 S/m, and wave attenuation is consequently not negligible. There are lots of models linking EM properties and snow properties (mostly snow density and liquid water content)[24]. Dry snow permittivity/velocity is dependent only on snow density while wet snow permittivity/velocity depends on snow density and liquid water content.

The typical slab avalanche situation, i.e., high density slab layer on top of thin low density weak layer, can be directly described by density changes and then by permittivity changes and consequently affected by EM

[24] Di Paolo, F. et al. (2018), Dry snow permittivity evaluation from density: A critical review, In 2018 17th International Conference on Ground Penetrating Radar (GPR) (pp. 1-5). IEEE.

wave propagation. Some examples of models linking permittivity of dry snow ε_R and dry snow density $\rho_{drysnow}$ are given below[25,26,27]:

$$\rho_{drysnow} = \frac{\epsilon_R - 1}{0.00183}$$
$$\rho_{drysnow} = \frac{1000\,(\sqrt{\epsilon_R} - 1)}{0.845}$$
$$\rho_{drysnow} = \frac{(\sqrt[3]{\epsilon_R} - 1)\rho_{ice}}{\sqrt[3]{\epsilon_{ice}} - 1}$$

where ρ_{ice}= 917 kg/m^3 and ε_{ice} = 3.5 are ice density and ice relative permittivity respectively.

For wet snow, a term dependent on the liquid water content (LWC) is added to the dry snow density. The permittivity of wet snow (ε_R) is then calculated either with an empirical equation (Frolov, 1999) or with an extended Looyenga equation such as:

$$\epsilon_R = \left(1 + 0.845\frac{\rho_{drysnow}}{1000}\right)^2 + 16.7LWC + 42.5LWC^2$$
$$\epsilon_R = \left[\frac{(\sqrt[3]{\epsilon_{ice}} - 1)\rho_{drysnow}}{\rho_{ice} + 1} + LWC\,(\sqrt[3]{\epsilon_{water}} - 1)\right]^3$$

Where LWC is the liquid water content in percentage (usually between 0 and 10 %) and ε_{water} is the relative permittivity of liquid (melt) water at 0 degrees celsius: ε_{water} = 86.

6.3 Operational Requirements

6.3.1 GPR technologies

Conventional GPR is using pulsed radar technology, i.e., that an ultrawideband pulse is generated and sent towards the subsurface. Reflected waves are recorded versus time. Frequency band is dependent on the central frequency of the source (Ricker) and is following a gaussian distribution. Several manufacturers are building RTS (real time sampling) radars that allows recording of much more than a single sample per transmitted pulse. The main advantage is that the signal to noise ratio is better, and the bandwidth of the signal is enlarged at the same time.

Step-frequency continuous wave (SFCW) radars are specific to only a couple of providers. They allow to cover a wide frequency band by sampling sinusoidal signal at several frequencies and converting in time domain with an inverse Fourier transform. The technology allows to make the most out of the recorded signals by selecting the frequency range needed for the specific application, and then avoiding limitations in resolution versus penetration depth that pulsed and RTS radar have. An alternative to SFCW radar is to combine pulsed radar antennas of several frequencies.

[25] Pasian, M. et al. (2019), Three-antennas FMCW radar for self-consistent snowpack monitoring, In 2019 13th European Conference on Antennas and Propagation (EuCAP) (pp. 1-4). IEEE.
[26] Frolov, A. D. and Macheret, Y. (1999), On dielectric properties of dry and wet snow, Hydrological processes, Vol. 13(12-13), pp. 1755-1760.
[27] Looyenga, H. (1965), Dielectric constants of heterogeneous mixtures, Physica, Vol. 31(3), pp. 401-406.

6.3.2 Challenges related to drone GPR operations

GPR antennas are usually designed to work in contact with the ground. Air coupled antennas exist but are more seldom than ground coupled antennas. Source radiation patterns and antenna footprint require careful design. For example, to avoid too much energy dispersion in the air, shielded or directional antenna are recommended. Cabrera and Bekic (2018)[28] give a good overview of the challenges for GPR airborne use. They especially explained that lots of EM energy is reflected at the air/ground interface, and this varies depending of the type of material (see Table 6). Snow and ice are the materials with the least reflection (respectively 7 and 28 %) making airborne GPR surveys very suitable.

Table 1

Material	Dielectric Perm.	Reflected energy at interface
Water	81	80%
Wet soils	20	64%
Typical soils	9	50%
Dry sand	6	42%
Ice	3	28%
Snow	1.3	7%

Table 6: percentage energy lost at air to ground interface (from Cabrera and Bekic, 2018)

Another challenge is related to the drone flights themselves. Early testing has shown that recording data between 2 and 3 m is the best compromise between flight safety and data quality. However, on steep slopes, flying close to the surface and following the terrain might be challenging in case of difficult flight conditions (wind or bad visibility). The challenge can be partially mitigated by implementing a laser or radar altimeter connected to the flight control unit.

6.4 Experimental Results

Figure 13 gives examples of two GPR profiles at Storlidalen, where extensive surveys have been carried out in winter 2022. A ground survey and several drone borne surveys have been recorded in wind loaded zone. The snow depth varies from 0 to 2.5m, increasing towards east along the slope. A detailed snowpit (white circle in the middle of the ground survey) has been dug and hand hardness has been recorded showing several melt crust layers between 1 and 1.5m depth. In the drone GPR data, we clearly observe the snow surface (drone is flying at 2m above ground level approximately) and the interface between snow and ground. Internal reflection events are also visible and especially the main one that we can associate with icy crusts observed in the snowpit. The main differences with the ground survey lie in the data quality, especially a better signal-to-noise ratio for ground survey, and better resolution for internal and shallow layers. The drone data are, as expected, of lower quality but the main layers are observable.

[28] Cabrera, R. A., & Bekic, G. (2018), Drone-borne ground-penetrating radar suitability for specific surveys: a comparative study of feature sizes versus antenna frequency and elevation over the ground, First Break, Vol. 36(8), pp. 83-89.

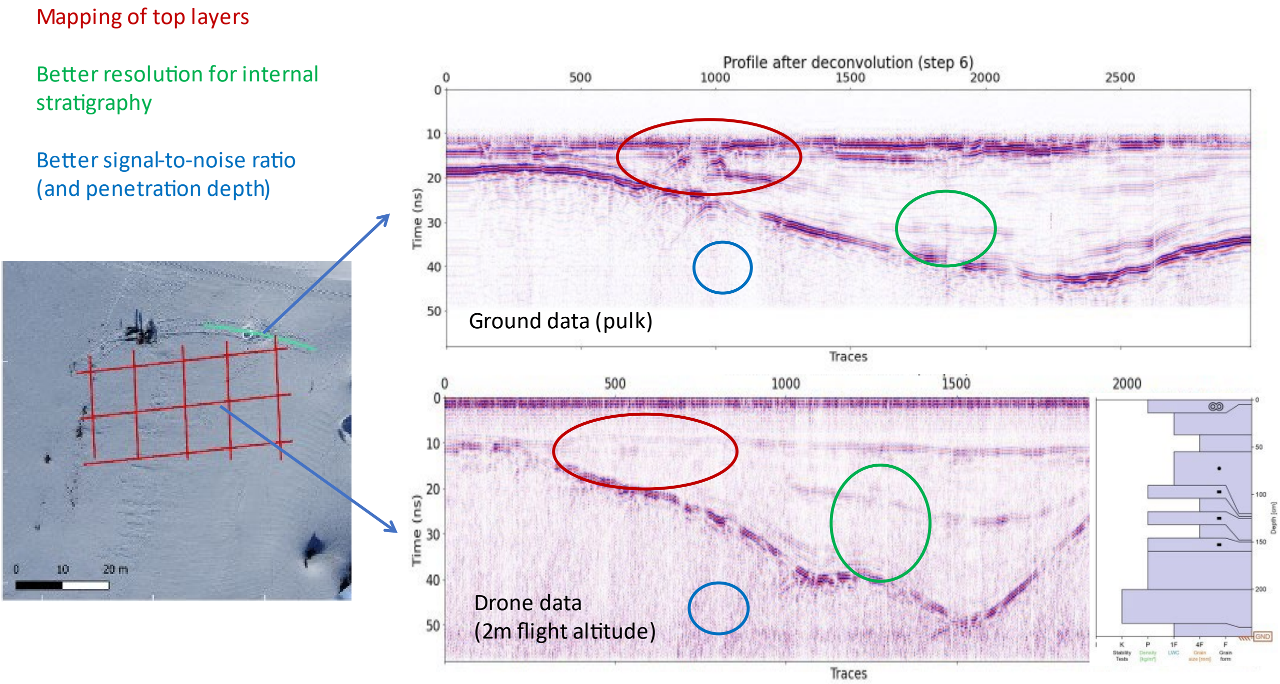

Figure 13: ground (top right) and drone (bottom) GPR profiles. The aerial photography on the left gives the location of the profiles while the the snowpit with hand hardness estimations are given on the bottom right.

7 Other Sensor Technologies

In this chapter, we describe a list of other possible sensors which can provide interesting information on snow surface and snowpack properties. The list is non-exhaustive.

7.1 Pyranometer for snow albedo

Albedo is the proportion of incoming incident energy/radiation which is reflected at the ground surface back towards the atmosphere. In addition to large-scale effects on climate, the albedo of the snow cover is critical to calculate snow accumulation, melt-freeze cycles and internal snowpack temperature gradients. Pyranometer are sensors which measure the solar irradiance and are light and compact enough to be mounted on UAVs. Sproles et al. (2020)[29] demonstrate the use of a combination of upward and downward facing digital pyranometers (145 g weight, 310-2700 nm spectral range) mounted on a DJI Matrice 210 V2. The upward facing pyranometer measures the incoming irradiance while the downward facing sensor measures the reflected irradiance at the surface. The test surveys run in Montana in spring 2019 were successful and show that the spatial variability of the albedo is better described with such drone measurements (compared to space-borne measurements).

7.2 Snowlaserdrill for snow density

The SnowLaserDrill (SLD)[30,31] is an instrument developed by Martin Koßagk and colleagues at the Technical University in Dresden, Germany and tested by Marc Adams team (BFW, Austria). It consists of a melting laser, drilling a hole into the snow, and a second laser to measure how the melting progresses. Since there is a linear relationship between snow density and melting progress, a density profile of the snowpack can be generated via a thermal model from the velocity data of the borehole progress. The SLD is set atop the snowpack and typically set to bore vertically into the snow – therefore no digging is required. The achievable drilling depth and speed depends on laser output power and collimation of the beam, the current prototype can record density over approximately 1m of snow in 30 min.

Primary application of the SLD in the short- to mid-term are snow density measurements for avalanche protection and snow water equivalent measurements for dam operators. However, the long-term goal is being able to drill the ice crust of icy moons around Jupiter and Saturn to explore their composition. The surface of icy moons with cryovolcanism consists of loose ice deposits whose density distribution allows conclusions to be drawn about the formation of this crust.

The instrument was extensively tested in the lab, and field tested for the first-time in spring 2022 with additional tests in Austria and Svalbard in winter 2023. At its current stage of development, the SLD prototype is mobile but must be handled by two people and requires a 30 W power supply. However, it is intended as a precursor to a more compact, lightweight, robust and more easily transportable instrument. The aim of future field tests and development is to gear the SLD toward airborne applications as payload on-board UAV or on remote snow recording stations.

---

[29] Sproles, E. A. et al. (2020), Autonomous Aerial Vehicles (AAVs) as a Tool for Improving the Spatial Resolution of Snow Albedo Measurements in Mountainous Regions, Hydrology, Vol. 7(3), pp. 41.

[30] Koßagk M. et al. (2023), A Novel Laser-based Instrument for Estimating Depth-Resolved Snow Density - Part 1: Lab Experiments, ISSW Proceedings.

[31] Adams M. et al. (2023), A novel laser-based instrument for estimating depth-resolved snow density – Part 2: Field tests, ISSW Proceedings.

7.3 Synthetic aperture radar

Gamma Remote Sensing[32,33] developed compact portable L-band SAR (Synthetic Aperture Radar) which can be mounted on a drone.[34] They demonstrate the use of the radar mounted on a VTOL fuel-powered helicopter drone (18 kg payload) for glacier velocity measurements and slope stability assessment. The SAR system is a Frequency Modulated Continuous Wave (FMCW) radar with a frequency of 1.2 to 1.4 GHz and it weighs 7.65 kg. The data processing is using standard repeat-pass interferometry SAR (InSAR). Compared to terrestrial radar, there are challenges due to the moving system (require high precision GNSS and IMU) and operations and data quality can be difficult in case of wind.

Drone SAR system can be used similarly to a terrestrial SAR system, i.e. to monitor avalanche activity or fast moving landslides. Monitoring glide avalanche creep is also possible in theory. To some extent, it could be used to map snow depth changes if the drone flight is very accurately repeatable and if the snow depth changes are small (to avoid cycle-skipping in case of large phase delay). Drone photogrammetry or LiDAR is more relevant in this case.

7.4 RFID tags for snow thickness, snow density and temperature profiles

Radio-Frequency Identification (RFID) tags are low-cost, contactless and passive sensors which can be used for measurements of Snow Water Equivalent (SWE), snow depth and snowpack temperature. Usually used to identify goods remotely, RFID tag is constituted of an antenna and an ultra-low power microchip powered wirelessly by a reading device. The reading device/antenna interrogates the passive tag remotely and can be mounted on drone platforms. Such RFID tags are increasingly used in geosciences applications, including sediment transportation in rivers, temperature and soil moisture monitoring, landslide and rock displacements. Le Breton et al. (2022)[35] propose to use the phase delay due to propagation of EM waves between the reading antenna and the RFID tag to calculate an average wave velocity that can be converted to snow density and SWE. They are validating the system using RFID tags installed on a mast at different heights (corresponding to different snow depths when the snowpack is building over the season). In addition to EM phase delay, RFID tags allow to measure temperature, allowing to get some insights about temperature gradients in the snowpack.

RFID tags are very low-cost and passive sensors (do not need any power supply), so they can be placed, e.g. in summer, on the ground in avalanche starting zones, and be read from a drone mounted antenna over winter to derive accurate measurements of snow depth and effective snow density.

---

[32] Frey O. et al. (2019), Car-borne and UAV-borne mobile mapping of surface displacements with a compact repeat-pass interferometric SAR system at L-band, Proc. IEEE Int. Geosci. Remote Sens. Symp., pp. 274-277, https://doi.org/10.1109/IGARSS.2019.8897827

[33] Frey, O. and Werner, C. L. (2021), UAV-borne repeat-pass SAR interferometry and SAR tomography with a compact L-band SAR system, in Proc. Europ. Conf. Synthetic Aperture Radar, EUSAR, pp. 181-184, https://ieeexplore.ieee.org/document/9553573

[34] https://gamma-rs.ch/uploads/media/Instruments_Info/GAMMA_L-Band_SAR_information.pdf

[35] Le Breton M. et al. (2022), Monitoring snowpack SWE and temperature using RFID tags as wireless sensors, EGUsphere, pp.1-24.

7.5 Ambient noise monitoring for snow thickness and effective density

Measurements of seismic waves are common for avalanche monitoring and localization[36,37]. In addition, experimental and theoretical works demonstrated that mechanical properties of the snowpack which are affecting the seismic wave propagation in the snowpack can be directly linked to snow porosity (and consequently to snow density)[38]. Linking wave propagation observables (arrival times, amplitudes) to mechanical properties of the medium is actually not trivial in snow. Because such effects cannot be explained by elastic or visco-elastic effective models, one need to use poroelastic Biot models[39,40] which are predicting higher wave attenuation and dispersion (due to the presence to a slow compressional wave). While it is more complex to handle (more parameters to consider and frequency dependencies), the main advantage is that there is direct link between seismic observables and porosity of the material (here, the snow).

The difficulty with using seismic waves in snow is that active surveys requires the use of a seismic source, i.e. a system generating mechanical/seismic energy, usually an explosive.
An alternative to active surveys is to use passive seismic noise which is generated by environmental, human activities, ocean waves or earthquakes. In this case, the seismic sensors are recording ambient noise during a given period of time and applying cross-correlation interferometry concepts to get back effective properties of the medium under the seismic sensor array. One can take advantage of the dependency of seismic wave propagation to the mechanichal properties of the medium to get information on the snowpack. Such approach has been demonstrated in several recent studies:

- for imaging sea ice: using flexural waves, Serripierri et al. (2022)[41] estimates the effective Young's modulus, Poisson ratio and density of the sea ice layer in addition to its thickness and the variations during several days.
- for imaging firn layer in Antarctica: using surface waves (Rayleigh waves), Chaput et al. (2022)[42] estimates the seismic pressure and shear wave velocities and bulk density up to a depth of 100 m.
- for imaging snowpack thickness and density changes: Guillemot et al. (2021)[43] demonstrate that the effective seismic velocity recorded by passive seismic interferometry is varying due to snowfall events.

These recent experiments are promising but require the use of several seismic sensors (seismic array) in order to generate virtual sources by interferometry. To avoid any permanent array and take advantage of

---

[36] Van Herwijnen A and Schweizer J (2011), Monitoring avalanche activity using a seismic sensor, Cold Regions Science and Technology, Vol. 69(2-3), pp. 165–176.
[37] Lacroix, P. et al. (2012), Monitoring of snow avalanches using a seismic array: Location, speed estimation, and relationships to meteorological variables, J. Geophys. Res., Vol. 117, pp. F01034, doi:10.1029/2011JF002106.
[38] Sayers CM. (2021). Porosity dependence of elastic moduli of snow and firn. Journal of Glaciology. Vol. 67(265), pp. 788–796, https:// doi.org/10.1017/jog.2021.25.
[39] Sidler, R. (2015), A porosity-based Biot model for acoustic waves in snow, Journal of Glaciology, Vol. 61(228), pp.789-798.
[40] Capelli A. et al. (2016), Speed and attenuation of acoustic waves in snow: Laboratory experiments and modeling with Biot's theory, Cold Regions Science and Technology, Vol. 125, pp. 1-11.
[41] Serripierri, A. et al. (2022), Recovering and monitoring the thickness, density, and elastic properties of sea ice from seismic noise recorded in Svalbard, The Cryosphere, Vol. 16, pp. 2527–2543, https://doi.org/10.5194/tc-16-2527-2022, 2022.
[42] Chaput J. et al. (2022), Ambient high-frequency seismic surface waves in the firn column of central west Antarctica, Journal of Glaciology, Vol. 68(270), pp. 785–798, https://doi.org/10.1017/ jog.2021.135.
[43] Guillemot, A. et al. (2021), Effect of snowfall on changes in relative seismic velocity measured by ambient noise correlation, The Cryosphere, Vol. 15(12), pp. 5805-5817.

the recent development of light accelerometer sensors (MEMS)[44], this type of sensor can be mounted on a standard commercial drone. After an initial surface survey (LiDAR or photogrammetry) to build a DEM, we can select relevant and safe spots where the drone with seismic sensor can land. Then, after recording data (seismic ambient noise) for a given time (to be defined by modelling, probably around 10-20 minutes), the drone will take-off and record data at another spot. Recording data at several locations will allow to calculate effective mechanical properties of the snowpack (thickness, density, bulk and shear moduli). This type of approach is not validated and requires to be tested on the field.

8 Conclusions

This report gives an overview of the existing sensor that can be mounted on UAV platform and can provide information on the surface and subsurface of the snow cover. LiDAR and RGB cameras (for photogrammetry) are routinely used for imaging the snow surface and deriving snow height estimates and snow height changes over time. Multispectral cameras and thermal cameras are commonly used on UAV and could provide additional information on the snow surface e.g., grains size and moisture. GPR is conventional sensor for ground geophysics surveys whose lighter versions have recently been developed to be mounted on UAVs. GPR sensor has the possibility to provide information on the snowpack layering and the snow properties in addition to high-resolution snow height mapping. Finally, we present few sensors which can be mounted on UAV but are at an early stage of development. For example, the SnowLaserDrill sensor may allow to derive snow density logs while pyranometers can be useful to determine the albedo of the surface.

[44] Mougenot, D. et al. (2011), MEMS-based accelerometers: expectations and practical achievements, First Break, Vol. 29(2).

Statens vegvesen
Pb. 1010 Nordre Ål
2605 Lillehammer

Tlf: (+47) 22 07 30 00

firmapost@vegvesen.no

ISSN: 1893-1162

Tryggere, enklere og grønnere reisehverdag